Cell Tissue Res (1998) 293:165-171

REGULAR ARTICLE

Jan Fridén · Richard L. Lieber

Segmental muscle fiber lesions after repetitive eccentric contractions

Received: 4 March 1997/ Accepted: 3 February 1998

Abstract Immunohistochemical and electron-microscopic techniques were used to analyze the extensor digitorum longus muscles of New Zealand White rabbits 1 h, 1 day, 3, 7, and 28 days after repetitive eccentric contractions. Loss of the cytoskeletal protein desmin was the earliest manifestation of injury. Apart from 1 h post-exercise, all desmin-negative fibers stained positively with antibody to plasma fibronectin, indicating loss of cellular integrity accompanying cytoskeletal disruption. Fiber sizes were significantly increased from 1–7 days after exercise. The large (hyaline) fibers found in histological sections after repetitive eccentric contractions resulted from segmental hypercontraction of the fiber. This phenomenon occurred proximally and distally to plasma membrane lesions of the muscle fiber and necrosis and manifested itself as very short sarcomere lengths. Thus, in serial sections, staining characteristics, sizes and shapes of one and the same fiber often varied dramatically. We conclude that the following sequence of events occurs: cytoskeletal disruptions, loss of myofibrillar registry, i.e., Z-disk streaming and A-band disorganization, and loss of cell integrity as manifested by intracellular plasma fibronectin stain, hypercontracted regions, and invasion of cells. When a fiber is disrupted, the remaining intact fibers apparently take up the tension put on the muscle and later fewer fibers are subjected to eccentric contractions.

This work was supported by the Swedish Medical Research Council, the Swedish National Centre for Research in Sports, the Veterans Administration, and NIH grant AR40050

J. Fridén
Department of Hand Surgery, Sahlgrenska University Hospital, University of Göteborg, Göteborg, Sweden
Tel.: +46-31-601000; Fax: +46-31-820589;
e-mail: jan.friden@orthop.gu.se

R. L. Lieber
Department of Orthopaedics and Biomedical Sciences Graduate Group, University of California and Veterans Administration Medical Centers, San Diego, USA

Key words Muscle injury · Cytoskeleton · Sarcomere organisation · Immunohistochemistry · Ultrastructure · Rabbit (New Zealand White)

Introduction

In a number of previous studies of muscle injury, fibers with abnormal shapes and sizes have been used as morphological indices of acute exercise-induced muscle injury (Armstrong et al. 1983; Fridén et al. 1991; Lieber and Fridén 1988; Lieber et al. 1991; McCully and Faulkner 1985). This information is derived from routine histological staining. However, a better understanding of the proteins or enzymes involved in this process and the fate of the distorted fibers is required to increase our knowledge of damage mechanisms and events. Fibers with cross-sectional areas about three-times normal (21 000–28 000 μm^2) have been observed (Fridén et al. 1991; Lieber and Fridén 1988) in rabbit tibialis anterior muscle (TA) shortly after eccentric exercise (Lieber et al. 1991). All such fibers stain weakly for NADH, heavily for ATPase at pH 10.3, and strongly for fast-twitch myosin heavy chains and have thus been identified as fast-twitch glycolytic (FG) fibers. Furthermore, many of these large fibers contain intracellular deposits of plasma fibronectin, indicating a membrane lesion (Fridén et al. 1991). The specific cellular proteins involved in injury and their distribution are not known. We have suggested that the large fibers represent swollen or perhaps hypercontracted fibers subsequently undergoing necrosis and that relative lack of oxidative capacity is a factor in the selective vulnerability of the FG fibers (Lieber and Fridén 1988; Lieber et al. 1991). Our previous studies were not designed to assess the structural or metabolic features of these fibers. Therefore, the current study combines immunohistochemical and electron-microscopic techniques to define the three-dimensional morphological characteristics of these very large fibers. We have used a desmin antibody to assess the structural integrity of the exosarcomeric cytoskeleton

(Thornell and Price 1991), a fibronectin antibody to probe the integrity of the cell membrane (Vartio et al. 1987), and a titin antibody to identify structural abnormalities in the endosarcomeric cytoskeleton (Horowits and Podolsky 1987).

Materials and methods

Experimental model

The extensor digitorum longus (EDL) muscles of New Zealand White rabbits (mass=3.2±0.04 kg) were chosen because of their accessibility and the observation that large structural changes occur in this muscle after a single bout of eccentric exercise (Lieber et al. 1994). Animal care adhered to the NIH Guide for the Care and Use of Laboratory Animals and was approved by the UCSD Committee on Care and Use of Laboratory Animals.

Muscle functional properties were measured prior to experimental treatment and at one recovery time period between 1 and 28 days after treatment (Lieber et al. 1994). After the initial torque was measured, animals were either eccentrically or isometrically exercised noninvasively for 30 min (see below). The isometric group was included to provide an estimate of the torque decline caused simply by 30 min of repetitive stimulation without fiber injury. After the specified recovery period, contractile properties were again recorded.

Noninvasive treatment

Rabbits were anesthetized by a subcutaneous injection of a ketamine-xylazine-acepromazine cocktail (50, 5, and 1 mg/kg body mass, respectively) and maintained on halothane anesthesia (2%, 1 l/min). Heart and respiratory rates were monitored qualitatively throughout testing.

A dual-mode servomotor (Cambridge Technology model 6400, Cambridge, Mass.) with an adjustable foot plate attached to the motor arm measured the dorsiflexion torque during muscle activation (Lieber et al. 1991). The motor was calibrated by hanging known masses onto the foot plate at measured distances from the motor arm axis of rotation (accuracy: ±2%; error: 0.65±0.20%). The center of rotation of the rabbit ankle joint was aligned with the axis of rotation of the motor arm. Tibiotarsal and femorotibial angles were set to 100° and 90°, respectively, by using a goniometer. Twitch threshold voltage was determined by activating the peroneal nerve via subcutaneous needle electrodes. Threshold voltages below approximately 35 V, which corresponded to 3.5 mA, indicated accurate electrode placement. Voltage was then increased until peak twitch torque was reached. Subsequent tests were made at 2–3 times this maximal voltage to ensure complete activation of the dorsiflexor muscles. Torque was measured during twitch and tetanic contractions. Stimulation frequencies of 5, 10, 15, 20, 40, 60, 80, 100, and 200 Hz were chosen to minimize muscle fatigue while generating the force-frequency relationship. Maximal tetanic torque was defined as the peak of the force-frequency relationship, which occurred between 100 and 200 Hz for all rabbits tested.

For noninvasive eccentric exercise treatment, the ankle was moved from about 100° to 70° over a 400 ms period (stretch) and then returned to the starting position (shorten). The stretching movement during activation provided the eccentric exercise for both TA and EDL muscles. This pattern was repeated every 2 s for 30 min, resulting in 900 cyclic eccentric contractions.

After the appropriate experimental time interval, the animal was again anesthetized, and the EDL muscle was removed. A segment from the midportion (approximately 1 cm) of the muscle was used for analysis. Care was taken to sample muscles from as identical regions as possible. The samples were placed in OCT embedding medium (Miles Laboratories, Naperville, Ill., USA), with their fibers perpendicular to the surface of a piece of cardboard, and frozen in nitrogen-cooled isopentane.

Histochemistry

Cross sections (8 µm thick) were cut on a cryostat at –25°C (Reichert Jung, 2800 Frigocut, Austria). Serial sections were stained with hematoxylin and eosin for routine histological analysis, for NADH, and for myofibrillar ATPase activity after preincubations at pH 4.3, 4.6, and 10.3. Muscle fibers were typed into type 1, 2A, 2B, 2AB, and 2C according to a modification of the method of Staron and Pette (1986).

Immunohistochemistry

Cryosections were immunostained with the following antibodies: (1) against laminin (Novocastra Laboratories, Newcastle, UK) to visualize the basal lamina of the fibers (Sanes and Cheney 1982); (2) against fibronectin (monoclonal mouse antibody reacting with the cellular and plasma forms, courtesy of Prof. T. Vartio) to detect intracellular fibronectin (Vartio et al. 1987) indicative of membrane lesions; (3) against vimentin (human monoclonal antibody, Novocastra) to demonstrate inflammatory cells (Lazarides 1982); (4) against desmin (monoclonal mouse anti-human clone D33, from Dako, Glostrum, Denmark) for evaluation of the structural integrity of the cytoskeletal network (Thornell et al. 1985); and (5) against titin (Horowits and Podolsky 1987) to identify structural abnormalities in the endosarcomeric cytoskeleton. Antibody binding was visualized by the indirect peroxidase-antiperoxidase technique (Dakopatts, Copenhagen, Denmark; Sternberger 1979).

Morphometry

After fiber typing, fiber areas, maximum and minimum diameters, and perimeters in laminin-stained sections were measured by means of an interactive image analysis system (IBAS, Kontron, Eching Munich, Germany) connected to a Zeiss Axiophot light microscope (Zeiss, Germany) equipped with an MTI tube camera (DAGE-MTI, Michigan City, Ind., USA). Measurements were made by using a calibrated digitizing pad in conjunction with a computer-controlled morphometry program (IBAS, Kontron). All measurements were made blind to the experimental treatment. The coefficient of variation for repeated measurements of areas was 1.7%. Variability in calibration was less than 1% for measurements between separate digitizing sessions.

Electron microscopy

Muscles were fixed by immersion in 2.5% phosphate-buffered glutaraldehyde (0.1 M buffer adjusted to pH 7.4). The mechanically undamaged portion of the biopsy was transversely cut into slices approximately 1 mm thick. From these slices, 8–10 tissue blocks were post-fixed for 2 h in 1% osmium tetroxide, dehydrated in graded concentrations of ethanol, and infiltrated with Spurr's resin. Blocks were oriented so that muscle fibers could be sectioned either longitudinally or transversely.

Three tissue blocks from three specimens were chosen at random. Each was transversely oriented and semithin-sectioned (1 µm) for standard light-microscopic analysis. Fibers of extreme sizes were observed in cross section, after which the same specimen was tilted and longitudinally sectioned through the same fibers.

From the transverse and longitudinal survey, sections containing abnormally sized fibers (one region per section) were selected, trimmed, and sectioned for EM. Section thickness was kept as close to 60 nm as possible. From each of the longitudinal sections, 6–8 low-magnification micrographs (×1000) were mounted together to reconstruct the longitudinal muscle fiber morphology.

Fibers were classified as type 1 or type 2, with the subdivision of type 2 into type 2A or type B according to previously defined criteria (Fridén et al. 1988). Thus, fibers with M-bands showing all five M-bridges of equal density, were classified as type 1 fibers. All other fibers were termed type 2. From these fibers, those with the three mid-

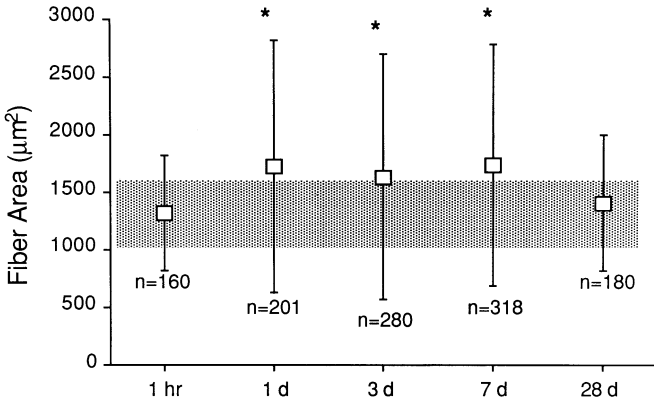

Fig. 1 Cross-sectional areas (mean±SD) of EDL fibers at various times after eccentric exercise. Fiber sizes were increased at 1–7 days. *Shaded band* Mean±SD for controls, **P*<0.05

dle M-bridges clearly visible but the two outer ones relatively less distinct were termed type 2A fibers. Fibers with only three middle M-bridges visible were termed type 2B. The reliability of this fiber-type discrimination technique has been demonstrated previously (Sjöström et al. 1982).

Results

Light microscopy

Various degrees of fiber disintegration and variable fiber sizes were observed. Whereas the vast majority (92%) of abnormal fibers were identified as type 2B, 8% were classified as type 2AB. Fiber areas varied between different post-exercise times. Thus, the fibers were significantly larger at 1–7 days after treatment compared with controls (Fig. 1).

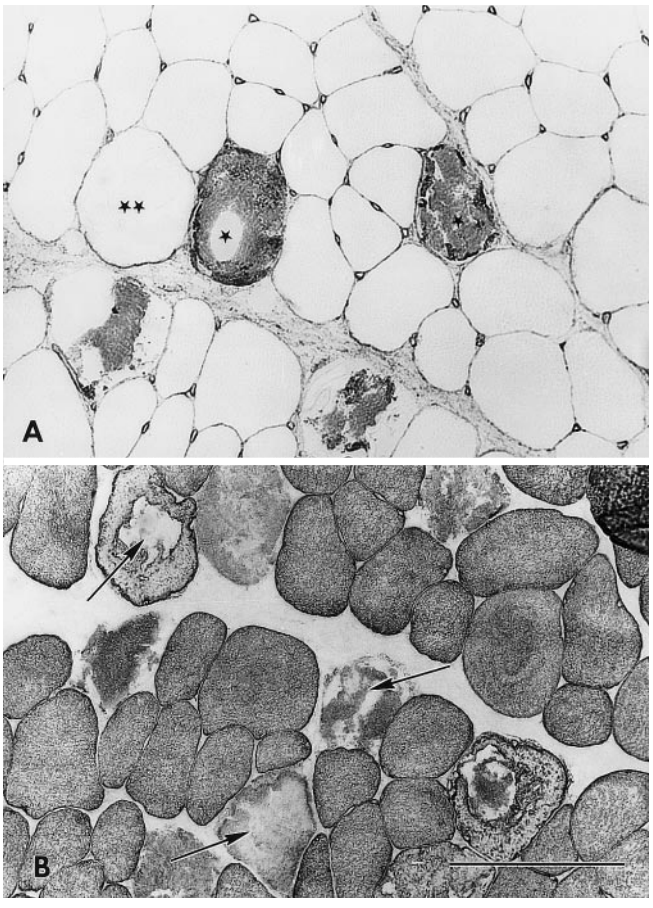

Fig. 2A, B Injured EDL muscle 3 days after eccentric exercise. **A** Fibronectin antibody. **B** Desmin antibody. *Arrows* Injured fibers in which desmin staining is lost. Fibers permitting the entrance of extracellular fibronectin into the cell (*) are considered more severely damaged; those excluding fibronectin (**) are less damaged. *Bar* 100 µm

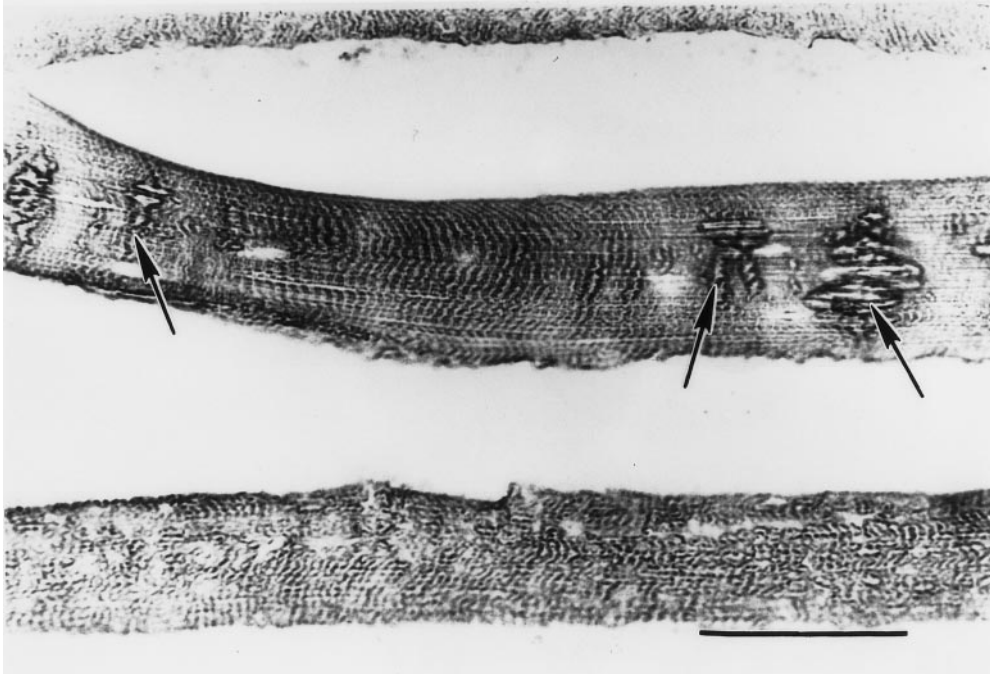

Fig. 3 Titin immunoreactivity in a longitudinal section of EDL muscle, 1 day after eccentric contractions. Disturbances of the sarcomere lattice are observed. Sarcomere lengths and thus fiber diameter vary along the damaged fibers. *Bar* 50 µm

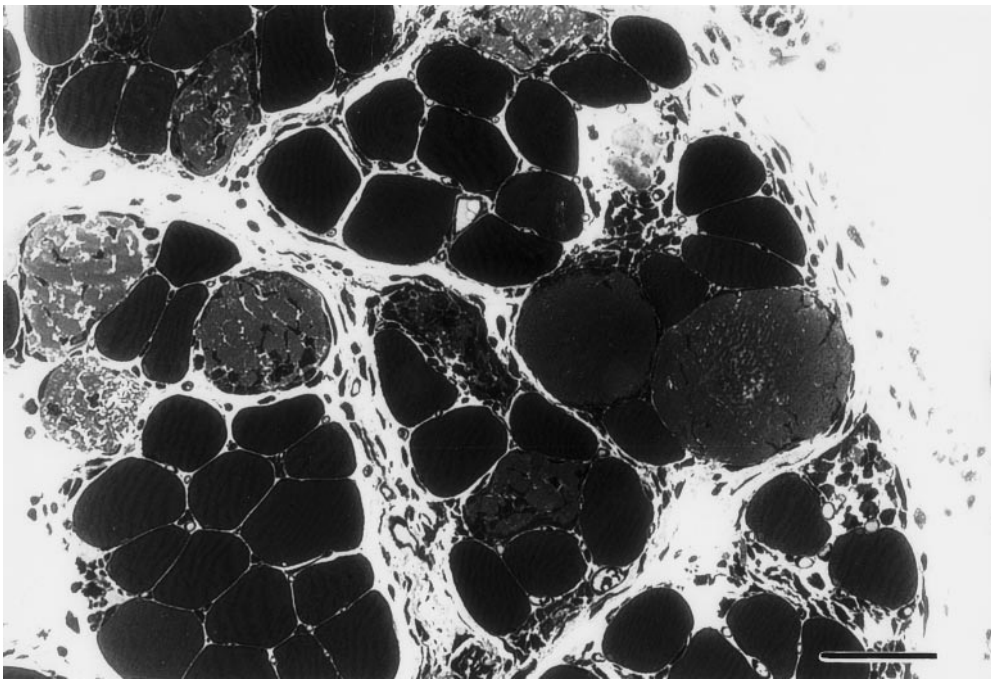

Fig. 4 Toluidine-blue-stained cross sections of EDL fibers, 3 days after eccentric exercise. A considerable number of the fibers are of abnormal shapes and sizes. Fibers at different stages of degeneration and regeneration are present. *Bar* 50 μm

Immunohistochemistry

Infrafiber localization of fibronectin was observed 1 h, 1 day, 3 days, and infrequently at 7 days after exercise (Fig. 2A). Many of the large fibers totally or partially lacked desmin immunoreactivity (Fig. 2B) in samples taken at all time points except after 28 days, when desmin-negative fibers occurred only occasionally. All degrees of desmin loss were observed. In the 1-h post-exercise biopsies, remnants of desmin were often surrounded by an incomplete or shrunken fiber membrane as shown by fibronectin staining. At 1 and 3 days post-exercise, desmin was absent in the majority of the large fibers in some parts of the muscle, but the loss was scattered in other parts.

The anti-titin-stained longitudinal sections consistently showed disturbances of the regular titin lattice of the sarcomere (Fig. 3). Regions with loss of stain were found next to normal regions. In less severe lesions, isolated sarcomeres were affected, although several myofibrils across the fiber were generally damaged. Sarcomere lengths thus varied significantly along the fibers with damaged titin lattices.

Low-magnification micrographs of toluidine-blue-stained cross sections revealed a significant portion of the fiber population with abnormal shapes and staining intensities (Fig. 4). Numerous large fibers were observed. No nonmuscle cells were found within the fibers 1 h post-exercise, but an average of 22%, 43%, and 16% of the fibers were infiltrated with mononuclear cells 1, 3, and 7 days after eccentric exercise. The frequency of infiltrating cells in sectioned fibers ranged from a single inflammatory cell to fibers completely filled with nonmuscle cells. No infiltrating cells were observed in muscles examined 28 days post-exercise.

The same large fibers that we examined in the cross sections could be readily identified in the toluidine-blue-stained longitudinal sections. The 1-h and 3-day post-exercise biopsies were selected for closer analysis. Complete analyses of the morphology of three fibers in longitudinal sections covering more than 3000 μm (approximately 300 sections) were performed. In the thick (corresponding to cross-sectioned large fibers) segments of these fibers, sarcomere length was 0.9±0.2 (SD) μm compared with 2.5±0.3 μm in the nonthickened fibers.

Electron microscopy

In cross sections of the large fibers, myofibrils were densely packed, although some myofibrils were often missing (Fig. 5A). The large fibers always contained thick filaments, although they were severely deranged. The typical A-band lattice was consistently distorted with missing filaments and abnormally oriented filaments. Z-disc lattices were never found, and even Z-disc material was absent.

In longitudinal sections of the large fibers, the thin and thick filaments were highly disorganized, and the remnants of the band pattern were wavy and consistently broken in many places (Fig. 5B). Sarcoplasmic reticulum and T-tubules were either normal or dilated in the biopsies taken 1 h post-exercise, but they appeared rounded and with an increased and often granular density in biopsies taken later after exercise (Fridén and Lieber 1996). Mitochondria were few, rounded, less electron-dense than normal, and with hardly discernable cristae.

Large fibers always became thinner at variable distances from the plane of cross sections in which they were identified. In the enlarged part of the fiber, the myofibrils and the sarcolemma generally remained visible, but in the adjacent

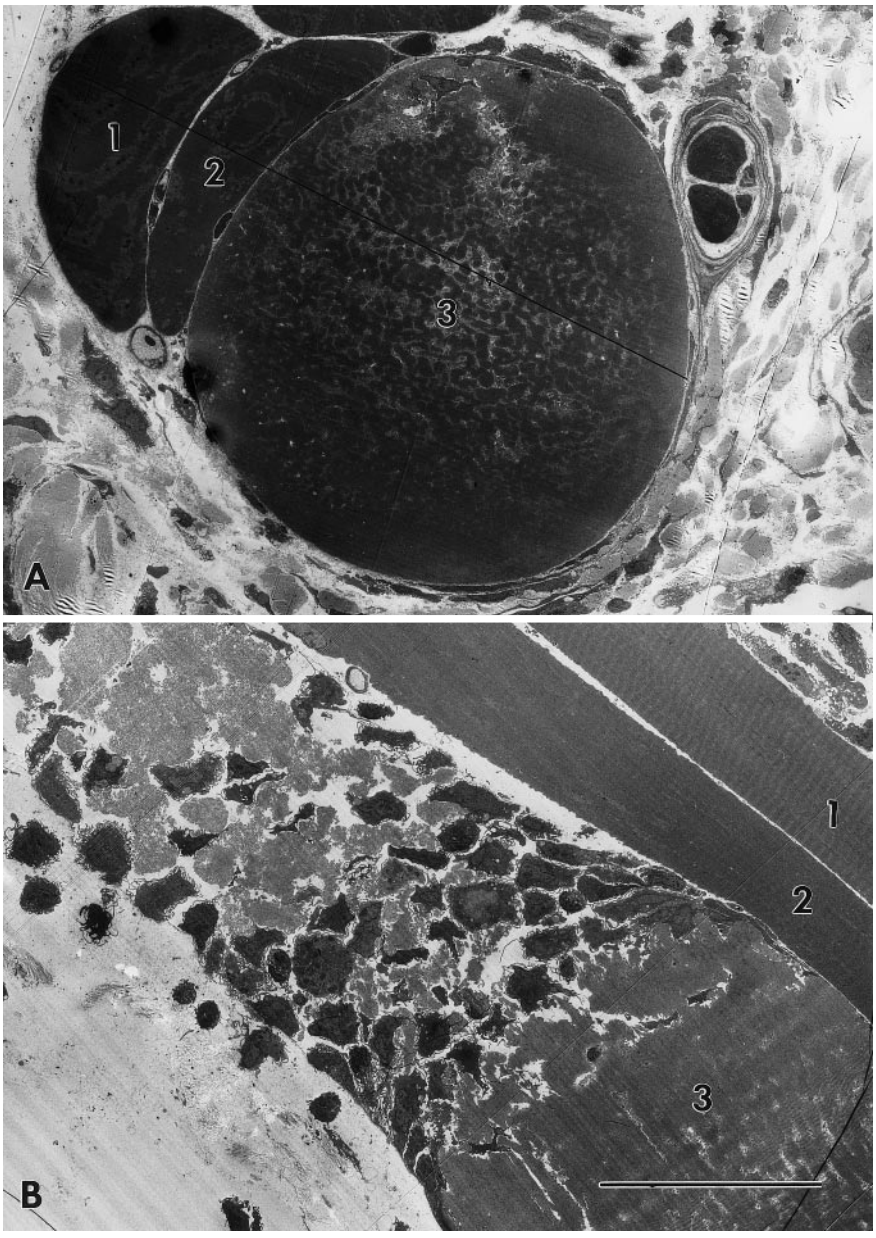

Fig. 5A Cross section of muscle showing an enlarged fiber (*3*) and two normal fibers (*1, 2*). **B** Longitudinal section (along the plane indicated in **A**) of muscle showing the inflammatory process that leads to enlarged fiber type and size variation. Enlarged fibers represent „supercontracted“ cells being digested by inflammatory cells a short distance away. *Bar* 50 µm

thinner portions, myofibrils were separated and often absent. Still further from the enlargement, the fiber regained its contractile elements, and myofibrils became increasingly densely packed. At variable distances from the enlarged zones, the fibers either regained their normal thickness or again became significantly wider than neighboring „normal“ fibers. At the junction between enlarged and thinned portions (Fig. 6, between regions A and B), invading cells were found, but to a much lesser extent than in the thin region. In the thinned region (Fig. 6, region B), the plasma membrane was only infrequently intact and numerous macrophages were always present at 3 days post-exercise.

Discussion

This study shows that the large muscle fibers found in histological sections after repetitive eccentric contractions represent segmental areas of muscle fiber hypercontraction. This phenomenon occurs adjacent to fiber plasma membrane lesions and is associated with very short sarcomere lengths. We conclude that differences in the number of large fibers between sections is random, because the structural integrity of individual fibers is broken at many points and thus cross-sectional size is variable along the fiber length. The sarcomere length is determined by the proximity of the section to the enlarged zones. Therefore, in serial sections, the staining characteristics, size, and shape of one and the same fiber may vary considerably.

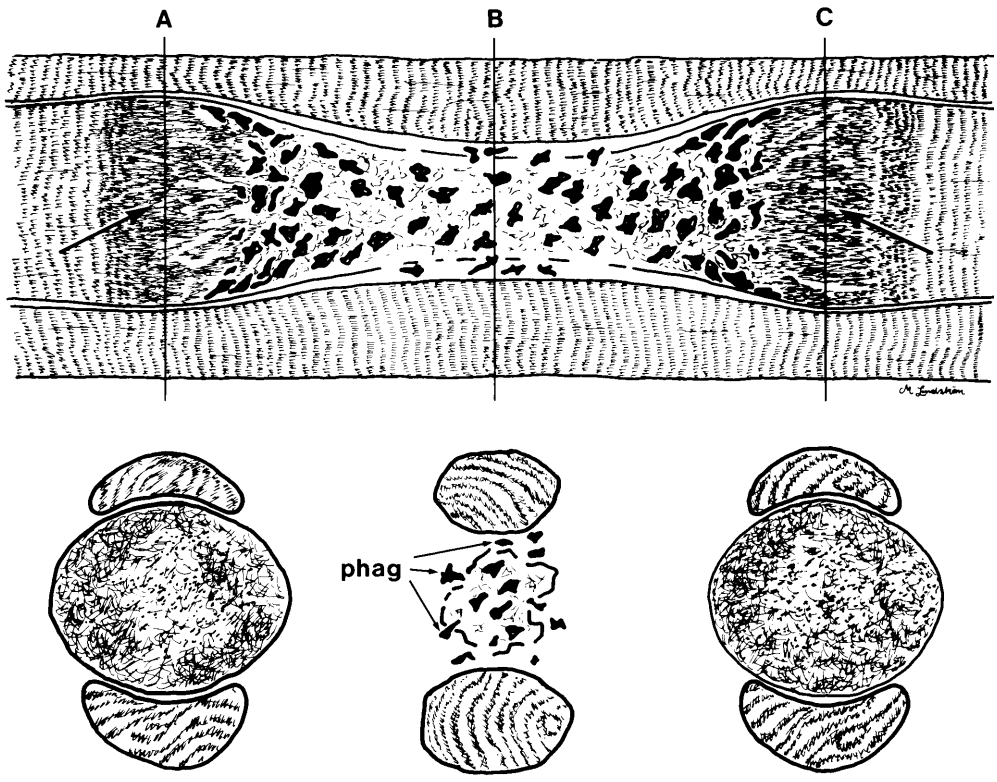

Fig. 6 Schematic drawing of longitudinal (*top*) and cross (*bottom*) sections of a muscle fiber with segmental damage surrounded by two normal fibers. *Vertical lines* Plane of cross sections. Hypercontraction zones (*arrow*) are bilateral to the necrotic zone. In the region of necrosis, phagocytes (*phag*) are present both within and outside the partially damaged muscle fiber membrane. The hypercontraction zones displace and compress the adjacent fibers, but in the region of lesion, these normal fibers taper along the damaged and narrow fiber

In light of the marked cellular infiltration observed in our study, it is surprising that Faulkner et al. (1989) have found no evidence of infiltration 24 h after exercise in muscles actively lengthened in a similar experimental procedure in rats. This may very well result from their use of relatively insensitive morphological methods (hematoxylin and eosin) without longitudinal sections and with no evaluation of the endosarcomeric cytoskeleton, which seems to be particularly vulnerable to eccentric forces. Our observations of segmental necrosis emphasizes the risk of missing fiber injuries unless numerous serial sections are observed. The segmental or focal nature of the damage in parallel with zones of hypercontraction have previously been described in various muscle diseases (Schmalbruch 1973, 1975). Focal degeneration, although without hypercontraction zones, has also been reported to result from heavy exercise in rats (Kuipers et al. 1983).

Lieber et al. (1991) have found variable fiber sizes in histological sections of biopsies 1 h after eccentric exercise. The current study confirms the finding of (Stauber et al. 1988) that this morphological feature is even more pronounced at subsequent time points. Our findings also demonstrate that fiber injuries may manifest as loss of anti-desmin immunoreactivity but without sarcolemma disruption. These fibers presumably correspond to the previously reported immediate ultrastructural consequence of eccentric load with distortion of the alignment of the A- and I-bands, irregular Z-discs, and slippage of the thick filaments out of the thin filament lattice (Dix and Eisenberg 1991; Lieber et al. 1991, 1996). The region affected may very well occur in foci in which the sarcolemma is intact, as shown by the exclusion of fibronectin. It is not likely that injuries occur at multiple sites in the same fiber because, once a fiber is disrupted, the remaining intact fibers supposedly take up the tension put on the muscle. On the other hand, a focally damaged fiber may function normally, because longitudinal and radial intermediate filaments span the injured segments and may transmit tension around the lesion and to neighboring fibers (Street 1983; Wang and Ramirez-Mitchell 1983).

The existence of disorganized sarcomeres (abnormal titin staining) early after the damage event implies that titin molecules have been primarily or secondarily damaged. Titin is a controller of filament assembly (Horowits and Podolsky 1987) and a single titin molecule spans from the Z-band to the M-band in vertebrate striated muscle (Fürst et al. 1988). The attachment of titin molecules to the Z-disk is interesting in the light of data establishing that the Z-disk is the primary site of injury in response to lengthening contractions (Newham et al. 1983; Fridén 1984). Based on this juxtaposition of numerous structural proteins, we suggest that mechanical imbalance between adjacent sarcomeres is a potential factor in the damage caused by eccentric contractions. Slight differences in length and velocity pose no threat to adjacent sarcomeres during muscle shortening, because the force-velocity relationship near zero velocity for muscle shortening is not very steep. However, because of the steepness of the lengthening portion of the force-velocity relationship, the force in adjacent sarcomeres during lengthening may vary by more than 50% (Fridén and Lieber 1992). It would, therefore, not be surprising for an actin filament to experience dramatically different forces on each of its ends. This would place directional stress on the Z-disk; such an imbalance could lead to Z-disk streaming,

which would be transmitted to the titin filaments thus causing disorganization of thick filament registry.

The tissue disruption in response to eccentric contractions is seen immediately after the termination of exercise (Armstrong et al. 1983; Newham et al. 1983; Fridén 1984). The lesion increases in size at 24 h and reaches its peak at 48 h (Armstrong et al. 1983; Fridén 1984; McCully and Faulkner 1985). The mechanism for the exacerbation of the initial injury is supposed to be the activation of lysosomal enzymes from neutrophils and platelets (Smith 1991). This is evidently the case in this study where the accumulation of phagocytotic cells is notable during segmental necrosis from 1–3 days after the damaging exercise. The process of the restoration of cytoskeletal and contractile protein morphology, including the restoration of sarcomere lengths after this type of injury, requires further investigation.

Acknowledgements The authors gratefully acknowledge the assistance of Ulla Hedlund and Professor Lars-Eric Thornell for providing antibodies and for valuable discussions.

References

Armstrong RB, Ogilvie RW, Schwane JA (1983) Eccentric exercise-induced injury to rat skeletal muscle. J Appl Physiol 54:80–93

Dix DJ, Eisenberg BR (1991) Redistribution of myosin heavy chain mRNA in the midregion of stretched muscle fibers. Cell Tissue Res 263:61–69

Faulkner JA, Jones DA, Round JM (1989) Injury to skeletal muscles of mice by force lengthening during contractions. Q J Exp Physiol 74:661–670

Fridén J (1984) Changes in human skeletal muscle induced by long term eccentric exercise. Cell Tissue Res 236:365–372

Fridén J, Lieber RL (1992) Structural and mechanical basis of exercise-induced muscle injury. Med Sci Sports Exerc 24:521–530

Fridén J, Lieber RL (1996) Ultrastructural evidence for loss of calcium homeostasis in exercised skeletal muscle. Acta Physiol Scand 158:381–382

Fridén J, Seger J, Ekblom B (1988) Sublethal muscle fiber injuries after high-tension anaerobic exercise. Eur J Appl Physiol 57:360–368

Fridén J, Lieber RL, Thornell LE (1991) Subtle indications of muscle damage following eccentric contractions. Acta Physiol Scand 142:523–524

Fürst DO, Osborn M, Nave R, Weber K (1988) The organization of titin filaments in the half-sarcomere revealed by monoclonal antibodies in immunoelectron microscopy: a map of ten nonrepetitive epitopes starting at the Z line extends close to the M line. J Cell Biol 106:1563–1572

Horowits R, Podolsky RJ (1987) The positional stability of thick filaments in activated skeletal muscle depends on sarcomere length: evidence for the role of titin filaments. J Cell Biol 105:2217–2223

Kuipers H, Drukker J, Frederik PM, Geurten P, Kranenburg GV (1983) Muscle degeneration after exercise in rats. Int J Sports Med 4:45–51

Lazarides E (1982) Intermediate filaments: a chemically heterogeneous, developmentally regulated class of proteins. Annu Rev Biochem 51:219–250

Lieber RL, Fridén J (1988) Selective damage of fast glycolytic muscle fibers with eccentric contraction of the rabbit tibialis anterior. Acta Physiol Scand 133:587–588

Lieber RL, McKee-Woodburn T, Fridén J (1991) Muscle damage induced by eccentric contractions of 25% strain. J Appl Physiol 70:2498–2507

Lieber RL, Schmitz MC, Mishra DK, Fridén J (1994) Contractile and cellular remodeling in rabbit skeletal muscle after cyclic eccentric contractions. J Appl Physiol 77:1926–1934

Lieber RL, Thornell L-E, Fridén J (1996) Cytoskeletal disruption occurs within 15 minutes of cyclic eccentric contractions. J Appl Physiol 80:278–284

McCully KK, Faulkner JA (1985) Injury to skeletal muscle fibers of mice following lengthening contractions. J Appl Physiol 59:119–126

Newham DH, Mcphail G, Mills KR, Edwards RHT (1983) Ultrastructural changes after concentric and eccentric contractions of human muscle. J Neurol Sci 61:109–122

Sanes JR, Cheney JM (1982) Laminin, fibronectin and collagen in synaptic and extrasynaptic portions of muscle fiber basement membrane. J Cell Biol 93:442–451

Schmalbruch H (1973) Contracture knots in normal and diseased muscle fibers. Brain 96:637–640

Schmalbruch H (1975) Segmental fiber breakdown and defects of the plasmalemma in diseased human muscles. Acta Neuropathol 33:129–141

Sjöström M, Ängquist KA, Bylund AC, Fridén J, Gustavsson L, Scherstén T (1982) Morphometric analysis of human muscle fibre types. Muscle Nerve 5:538–553

Smith L (1991) Acute inflammation: the underlying mechanism in delayed onset muscle soreness? Med Sci Sports Exerc 23:542–551

Staron RS, Pette D (1986) Correlation between myofibrillar ATPase activity and myosin heavy chain composition in rabbit muscle fibers. Histochemistry 86:19–23

Stauber WT, Fritz VK, Vogelbach DW, Dahlmann B (1988) Characterization of muscles injured by forced lengthening. I. Cellular infiltrates. Med Sci Sports Exerc 20:345–353

Sternberger LA (1979) Immunocytochemistry. Wiley, New York

Street SF (1983) Lateral transmission of tension in frog myofibers: a myofibrillar network and transverse cytoskeletal connections are possible transmitters. J Cell Physiol 114:346–364

Thornell L-E, Price M (1991) The cytoskeleton in muscle cells in relation to function. Biochem Soc Trans 19:1116–1120

Thornell L-E, Eriksson A, Johansson B, Kjorell U, Franke WW, Virtanen I, Lehto V-P (1985) Intermediate filament and associated proteins in heart Purkinje fibers: a membrane-myofibril anchored cytoskeletal system. Ann N Y Acad Sci 455:213–240

Vartio T, Laitinen L, Närvänen O, Cutolo M, Thornell L-E, Virtanen I (1987) Differential expression of the ED sequence-containing form of cellular fibronectin in embryonic and adult human tissues. J Cell Sci 88:419–430

Wang K, Ramirez-Mitchell R (1983) A network of transverse and longitudinal intermediate filaments is associated with sarcomeres of adult vertebrate skeletal muscle. J Cell Biol 96:562–570